SANDIA REPORT
SAND2010-7105
Unlimited Release
Printed October 2010

Aerosol Cluster Impact and Break-up: I. Model and Implementation

Jeremy B. Lechman

![Sandia National Laboratories logo] Sandia National Laboratories

Aerosol Cluster Impact and Break-up: Model and Implementation

Jeremy B. Lechman
[1]Nanoscale and Reactive Processes Department
Sandia National Laboratories
P.O. Box 5800
Albuquerque, New Mexico 87185-MS0836

Abstract

In this report a model for simulating aerosol cluster impact with rigid walls is presented. The model is based on JKR adhesion theory and is implemented as an enhancement to the granular (DEM) package within the LAMMPS code. The theory behind the model is outlined and preliminary results are shown.

CONTENTS

FIGURES

5

1. INTRODUCTION

Modeling the interactions of small particles is relevant to a number of applications (e.g., soils, powders, colloidal suspensions, etc.). Modeling the behavior of aerosol particles during agglomeration and cluster dynamics upon impact with a wall is of particular interest. In this report we describe preliminary efforts to develop and implement physical models for aerosol particle interactions. Future work will consist of deploying these models to simulate aerosol cluster behavior upon impact with a rigid wall for the purpose of developing relationships for impact speed and probability of stick/bounce/break-up as well as to assess the distribution of cluster sizes if break-up occurs. These relationships will be developed consistent with the need for inputs into system-level codes. Section 2 gives background and details on the physical model as well as implementations issues. Section 3 presents some preliminary results which lead to discussion in Section 4 of future plans.

2. MODEL AND IMPLENTATION DETAILS

2.1. Adhesion Model

Following the work of Chokshi et al. [1] a number of researchers (e.g., [2-7]) have used particle-based techniques for investigating coagulation/agglomeration of small particles. What each of these has in common is that their physical models for the interaction of pairs of aerosol particles in the direction normal to the point of contact between the particles are derived from JKR theory [8]. JKR theory [8] combines Hertz's analysis of elastic deformation of contacting spheres with a constant attractive adhesive force when particles are in contact. The resulting equation for the magnitude of the normal force between contacting spheres of identical material and size is

$$F_n = \frac{8Ea^3}{3d(1-v^2)} - 2\pi a^2 \sqrt{\frac{2\gamma E}{\pi a(1-v^2)}} \qquad (1)$$

where E is the Young's Modulus, v is the Poisson ratio, γ is the surface energy per unit area, $d=2R$ is the diameter of the particle, and a is the radius of the contact circle between the spheres. The first term on the R.H.S. is the standard Hertz result. The second term is the force due to the surface adhesion of the particles. Equation (1) gives the relationship between the force and the contact circle radius for identical spheres; although the results can be generalized to convex particles of differing size and materials. Furthermore, the contact radius a can be related to the relative displacement δ as

$$\frac{\delta}{\delta_c} = 6^{1/3}\left[2\left(\frac{a}{a_0}\right)^2 - \frac{4}{3}\left(\frac{a}{a_0}\right)^{1/2}\right] \qquad (2)$$

where the critical displacement at separation under tensile force is $\delta = -\delta_c$ with

$$\delta_c = \frac{2a_0^2}{d\,6^{1/3}}$$ (3)

and at equilibrium under zero applied force the contact circle radius

$$a_0 = \left(\frac{9\pi\gamma(1-v^2)d^2}{8E}\right)^{1/3}.$$ (4)

Note that for Hertzian contact without adhesion $\delta = 4a^2/d$. Equation (1) can be rewritten in a nondimensional form as

$$\frac{F_n}{F_c} = 4\left[\left(\frac{a}{a_0}\right)^3 - \left(\frac{a}{a_0}\right)^{3/2}\right]$$ (5)

where $F_c = 3\pi\gamma d/4$ is the force required to separate the adhered spheres. Figure 1 shows the value of the normal force as a function of the overlap, δ.
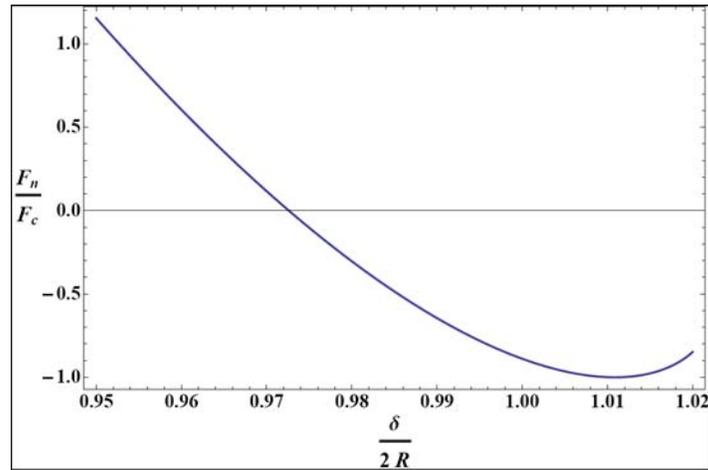

Figure 1: Normal force as a function of overlap, δ. Note: at contact, $\delta = 1.0$, force is non-zero due to adhesion while force for $\delta > 1.0$ applies only for separation after contact.

As noted above, many researchers seem to follow the work of Chokshi et al. in using the JKR theory of adhesion. However, alternatives have been proposed and debated in the literature most notably the DMT theory [9]. The differences between these were initially conceptual in formulating the problem, but led to very different predictions including different values of the pull-off force ($F_c=3\pi\gamma d/4$ for JKR and $F_c=\pi\gamma d$ for DMT). Later other approaches were developed to reconcile these discrepancies [10, 11]. From the later studies it was determined that JKR theory is appropriate for soft materials (i.e., low Young's Modulus) with high surface energies and large size whereas DMT theory is relevant for hard materials with low surface energies and small size; the key dimensionless parameter being

$$\kappa = \frac{32}{3\pi}\left(\frac{9d\gamma^2(1-v^2)^2}{2E^2z_0^3}\right)^{1/3} = \frac{32}{3\pi}\left(\frac{d}{z_0}\right)\left(\frac{\gamma}{k_n}\right)^{2/3}$$

(6)

where z_0 is the separation at which the attraction between the sphere surfaces is maximum. At high κ, JKR applies and low κ, DMT. The second equality follows from the discussion below (see equation (7)). Tsai et al. [12] have raised objections to JKR, DMT and the "unified" MYD theories. In particular, a formulation which is consistent with long-range van der Waals attraction between macroscopic spheres may require formulating the problem along the lines of [12]; although it is not entirely clear that this is necessary, at least initially. The JKR theory has been implemented in the current work as materials with high κ are being simulated and should it become necessary a change to DMT would be trivial. Questions about compatibility with the Hamaker equation for long-range van der Waals attraction have been set aside initially since we neglect these interactions at present; although they can be included trivially.

The above model is easily implemented in Discrete Element Codes which allow for simulating the many particle dynamics of cluster formation and behavior upon impact. DEM is the large particle analog of Molecular Dynamics. Newton's equations of motion are solved for each individual discrete particle. The positions of all the particles are specified as the initial condition for the simulation. Then, using equations (2) and (3) the radius of the contact circle can be found for any pair of particles that are in contact. That is, delaying the discussion of tangential contact forces until later, for identical spheres i and j in contact, we note that $\delta = d- r_{ij}$ where $r_{ij}=|\mathbf{r}_i-\mathbf{r}_j|$. Having calculated δ for a pair of particles, solving equation (2) for a now allows us to find the force acting between the particles via equations (4) and (5). The forces on each particle are summed and Netwon's First Law is integrated to get the velocities and integrated again to get the displacement. This is done for each particle. The particles are then moved and the new configuration allows us to repeat the process thereby iteratively evolving of the multi-particle dynamics.

Accordingly, equations (2-5) form the basis of the adhesive particle model implemented in Sandia's Large Atomic-Molecular Massively Parallel Simulator (LAMMPS) code. The current LAMMPS implementation of adhesive particle models is similar to previous work [5]; however a few differences in the details should be pointed out. As part of the general distribution, LAMMPS contains a "Granular" package that allows one to perform particle

simulations using the Discrete Element Method (DEM) [13]. LAMMPS's basic granular model for grain-grain interactions is based on the visco-elastic contact forces derived in [14]. These include a normal Hertzian elastic and a dissipative force describing the inelasticity of real materials. Note the dissipative force does not appear in equations (1) or (5). The tangential frictional forces are represented similarly using a Mindlin-type model [15]. In practice this amounts to a spring and a dashpot model for both the normal and tangential contact forces with the addition of a slider in the tangential model due to the Coulomb friction limit. To this basic model were added additional terms representing the surface adhesive force at contact as well as other terms, which restrict relative translation, rotation and twisting.

In the basic LAMMPS granular model, the user specified parameters for the normal interactions are the normal stiffness (with units of force/distance)

$$k_n = \frac{Ed}{3(1-\nu^2)} \tag{7}$$

and damping coefficient (with units of mass/time)

$$\eta_n = \frac{1}{3}\frac{(3\lambda-\zeta)^2}{(3\lambda+2\zeta)}\left[\frac{(1-2\nu)}{2\nu^2}\right]\sqrt{d\delta} \tag{8}$$

where ν is Poisson's ratio and ζ and λ are the shear and bulk "viscosities", respectively, of the material. **Note we have again assumed equal sized spheres of identical materials.** In the model of [5] following [15] the normal damping coefficient is written as

$$\eta_n = \alpha[2mk_n]^{1/2}\left(\frac{\delta}{d}\right)^{1/4} \tag{9}$$

with m the mass of the particle. Equation (9) is derived heuristically with the empirical coefficient α related to the coefficient of restitution. The visco-elastic model underlying equation (8) by contrast allows the damping coefficient to be specified independent of the normal stiffness – at least there is no explicit dependence on the normal stiffness even though there is an implicit dependence through the relative normal displacement δ. Similarly, the user specified parameters for the tangential interactions are the coefficient of friction

$$\mu \le \frac{F_t}{F_n} \tag{10}$$

where F_n and F_t are the normal and tangential force magnitudes, respectively. The tangential stiffness is defined by

$$k_t = \frac{E}{(2-\nu)(1+\nu)}\sqrt{d\delta} = \frac{2G}{2-\nu}\sqrt{d\delta} \tag{11}$$

where G is the shear modulus. Equation (11) is based on the analysis of Mindlin and Deresiecz for the case of no-slip [15]. Implied by equation (11) is the fact that the tangential force-displacement relationship depends on the relative normal displacement. Finally, and tangential damping coefficient can also be specified; however it has been ignored (i.e., set equal to zero) in the current work.

Given the above discussion, the magnitude of the total normal force acting on particles i and j in contact, again assuming identical particles, can be written as

$$\frac{F_{n,ij}}{F_c} = 4\left[\left(\frac{a}{a_0}\right)^3 - \left(\frac{a}{a_0}\right)^{3/2}\right] - \frac{4\eta_n}{3\pi\gamma d}(\mathbf{v}_{ij} \cdot \mathbf{n}_{ij}) \tag{12}$$

where $\delta(a)$ is given in equation (2) and $\mathbf{v}_{ij} = |\mathbf{v}_i - \mathbf{v}_j|$ is the relative velocity of the pair and $\mathbf{n}_{ij}$ the unit normal vector and the contact. The magnitude of the tangential force is given by

$$\frac{F_{t,ij}}{F_c} = \frac{4k_t\delta}{3\pi\gamma d} \tag{13}$$

where k_t is defined in equation (11) and the tangential force is limited by the adhesion analog of equation (10), namely

$$F_{t,ij} \leq \mu(F_{n,ij} + 2F_c). \tag{14}$$

Note it is more convenient to write the tangential force in terms of δ and not a as in equation (12). Recall that δ is the quantity calculated directly during the force determination; subsequently equation (2) is solved for a and used in (12). In fact, equation (2) is solved analytically (selecting the root that gives real values) and implemented in the code. The total force on particle i can now be written as

$$\mathbf{F}_i = \sum_{j \neq i} F_{n,ij}\mathbf{n} + F_{t,ij}\mathbf{t} \tag{15}$$

where **t** is the unit vector tangential to the contact and in the direction of sliding (**n** x **t** = *0*). Additional forces including long-range van der Walls attraction or electrostatic repulsion (i.e., DLVO-type forces) and forces due to particle-fluid interactions (Brownian, drag, etc.) are available in LAMMPS or by coupling LAMMPS to a fluid flow solver and can be included at a later date.

2.2. Sintered Particle Contact Constraint Model

In addition to the JKR adhesion which applies to the forces between particle pairs in contact, a model for sintered constraints between contacting particles has been implemented. In addition to the tangential and normal forces a torque between contacting particles is included. This model follows [5] and details can be found there. Here we outline some of its aspects in the LAMMPS implementation. The total torque on a particle *i* is given by

$$T_i = \sum_{j \neq i} RF_{n,ij}(\mathbf{n} \times \mathbf{t}) + T_{r,ij}(\mathbf{t_r} \times \mathbf{n}) + T_{t,ij}\mathbf{n} \tag{16}$$

where $\mathbf{t_r}$ is the unit vector tangential to the contact and in the direction of rolling, T_r is magnitude of the torque on the particle due to the rolling resistance and T_t is the magnitude of the torque due to resistance twisting of the particle about the contact normal. As mentioned, further details can be found in [5]. The twisting torque is limited by

$$M_t \leq -\frac{2}{3}\mu a(F_n + 2F_c) \tag{17}$$

while the rolling torque satisfies

$$M_r \leq k_r \xi_{crit} \tag{18}$$

where $k_r = 4F_c(a/a_0)^{3/2}$ is the rolling "stiffness" and ξ_{crit} is the is the critical rolling displacement [5] which is a user specified value. This sintered particle model can be used in conjunction with the JKR adhesion or the user can choose to perform simulations with JKR adhesion only.

3. PRELIMINARY RESULTS

In this section, the simulation setup and methods are described as well as showing some preliminary results.

3.1. Problem Statement and Formulation

As mentioned in the Introduction, the ultimate goal is to perform simulations to study aerosol cluster impact and break-up. Nominally, 20nm Ammonium Nitrate particles, idealized as

identical spheres, are the constituents of the clusters. Initially, gravity, long-range (i.e., non-contact) van der walls attraction and electrostatic repulsion between particles and wall, and interaction with a background fluid have been ignored. However, adhesion between the particles and the wall is accounted for. In order to perform the simulations the following steps must be taken:

- Generate initial fractal clusters
  - Grow randomly (diffusive cluster-cluster aggregation – DCCA) via Brownian/Langevin dynamics and adhesion model
  - Build directly with target fractal dimension (ballistic cluster-cluster aggregation-like models – BCCA)
- "Throw" clusters at flat, rigid wall varying impact velocity
  - Initially ignore fluid flow and particle-fluid coupling
  - Initially assume no random motion of particles, which may occur due to thermal, or turbulent fluctuations in the background fluid
- Characterize agglomerate response: bounce, collapse, change in fractal dimension, fracture: fracture probability and fragment size distribution, etc.
- Develop models to predict response based on agglomerate characteristics and impact conditions

In performing the simulations the flowing non-dimensional units will be used
- Length: $d = 1.0$
- Mass: $m = 1.0$
- Time: $\tau = \sqrt{d/g}$, where g is the acceleration of gravity, representing the time taken for a particle to fall its own diameter under the influence of gravity ($g = 1.0$ in non-dimensional units)
- Force: γd
- Energy: γd^2

A key dimensionless ratio is γ/k_n as can be seen by substituting equations (4) and (7) into equation (12) (see also equation (6) and the discussion concerning it). It should be noted at this point that although we have a direct relationship between elastic material properties of a material and k_n (equation (7)), for computational efficiency for very stiff materials (e.g., glass) the value of k_n used in the simulations is several orders of magnitude smaller than the value determined by equation (7). This is due to the stability of the time-stepping scheme where the timestep must satisfy $\delta t < \sqrt{m/k_n}$. Hence the larger k_n the smaller δt. Realizing this requires γ to be adjusted accordingly in the simulation while keeping the ratio γ/k_n equivalent to the physical value. Another key ratio for particle-particle (similar for particle-wall) collisions is

$$\lambda = \frac{2F_c \delta_c}{mv_0^2} = \frac{(3\pi)^{5/3}}{4*6^{1/3}}\left(\frac{\gamma}{k_n}\right)^{2/3}\left(\frac{\gamma d^2}{mv_0^2}\right) = \frac{(3\pi)^{5/3}}{4*6^{1/3}}\left(\frac{1}{c}\right)\left(\frac{\gamma}{k_n}\right)^{5/3} \quad (19)$$

where v_0 is the initial velocity of the particle (i.e., velocity prior to impact) and c is a constant related to converting the time units in the velocity to $\sqrt{m/k_n}$ which, according to the above,

originally had units of $\tau = \sqrt{d/g}$. Equation (19) is the ratio of adhesion energy to kinetic energy for a single particle. The value of this ratio is related to whether colliding particles will stick or not (ignoring inelastic dissipation in the collision) [1]. This ratio indicates that if γ is to be scaled while keeping the ratio γ/k_n constant then the velocity must be scaled as well to recover the correct stick or bounce behavior of the particle-particle (particle-wall) interaction.

3.2. Aerosol Cluster Formation

The initial conditions for a simulation of an aerosol cluster impacting a wall consists of specifying the geometry of the cluster. It is well known that the fractal dimension of the cluster describing its geometry depends on the agglomeration process [16, 17]. A couple approaches can be taken to build these initial fractal clusters. One can either simulate the exact formation process [e.g., 19, 20], or the clusters can be built by an algorithm which attempts to model the physical formation process [e.g., 18, cf. 6 and 7]. Since the former can be algorithmically and computationally intensive, the latter process will be adopted. Figure 2a shows a representative cluster of 4096 particles generated from an algorithm similar to [18]. Figure 2b shows the method for determining the fractal dimension from the scaling of the radius of gyration with number of constituent particles in the cluster. This algorithm yields clusters with fractal dimensions ~2.05. Modifications can be made to yield fractal dimensions ~1.91 [18]. Alternative algorithms can give clusters of arbitrary fractal dimensions.
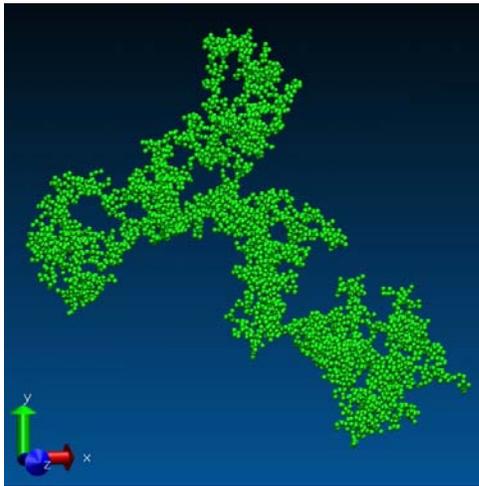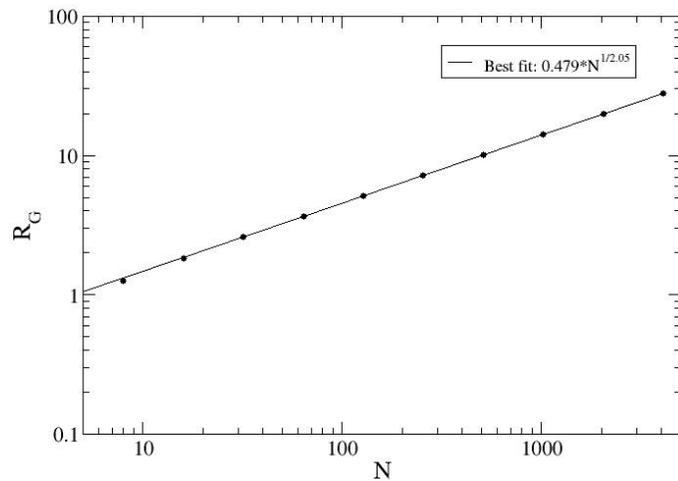

(a)   (b)

Figure 2: (a) Representative aerosol cluster formed by model cluster generator and (b) radius of gyration of cluster versus number of constituent particles.

In addition, as part of the validation of the for model described in section 2, Brownian Dynamics-like simulations were performed with particles interacting under influence of JKR forces only and with the sintering-like contact constraint model. Examples of particle clusters from these small simulations are shown in figure 3.
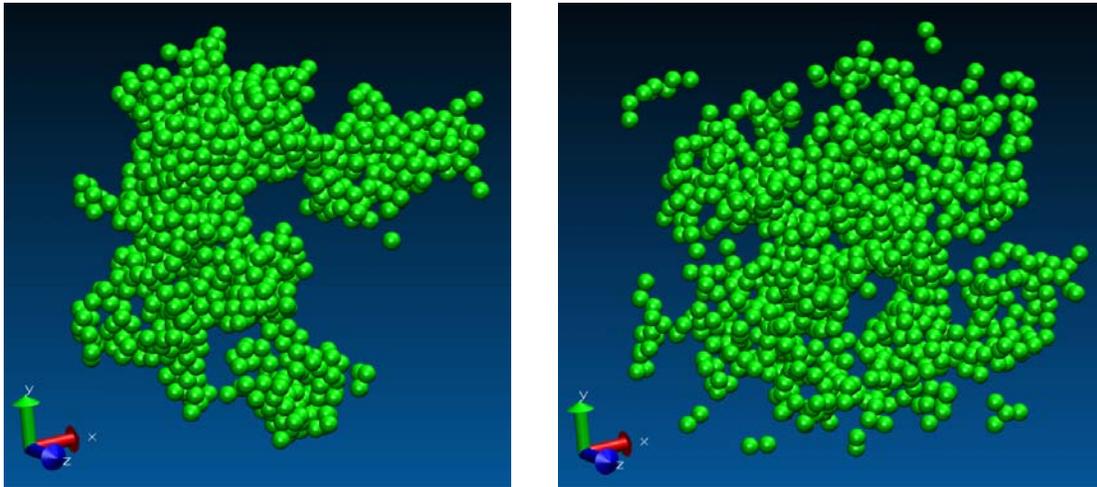
(a) **(b)**

Figure 3: Representative aerosol cluster formed by Brownian Dynamics simulations: (a) without the sintering model and (b) with the sinter model.

As pointed out in [19], finite size effects are very much preset in the simulations of which the clusters in figure 3 are representatives. However, it can still be clearly seen that the sintering constraints lead to a more open structure after the same number of time steps.

3.3. Cluster-wall Impact

Taking the cluster of figure 2, one can "throw" it against a flat, rigid wall and observe the behavior as in figure 4. The parameters for this simulation were $\gamma/k_n \sim 0.001$, $\mu = 0.5$ the initial impact velocity of the cluster was $1\ d/\tau$. There was no attractive interaction between the wall and the individual particles, but the Hertzian elastic and frictional interactions are the same between the grain-grain and grain-wall interactions. Although the snapshots end before rebound of the cluster from the wall impact, it can be seen that these parameters give a very ductile-like response with no cluster fracture/break-up.
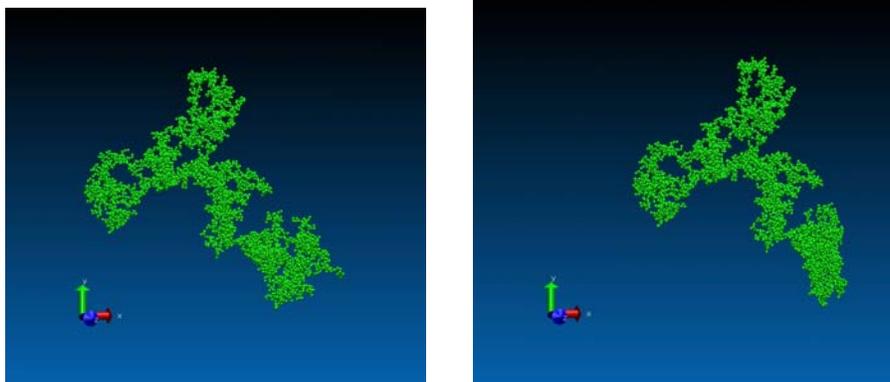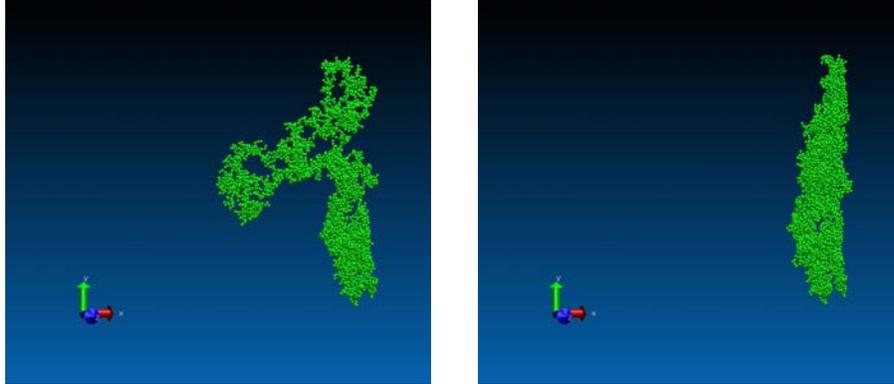
Figure 4: Snapshots of the cluster from Figure 2 impacting a flat, rigid wall.

4. CONCLUSIONS AND FUTURE WORK

Physical models for aerosol particle dynamics and adhesion have been implemented in Sandia National Laboratories' Large Atomic Molecular Massively Parallel Simulator. Preliminary results indicate that these models are functioning as expected. A full investigation of the problems remains for a later date.

5. REFERENCES

1. Chokshi, A., A. G. G. M. Tielens, and D. Hollenbach, *Dust Coagulation*, The Astorphysical Journal, 407:806-819, 1993.
2. Dominik, C. and A. G. G. M. Tielens, *The Physics of Dust Coagulation and the Structure of Dust Aggregates in Space*, The Astrophysical Journal, 480:647-673, 1997.
3. Marshall, J. S., *Particle Aggregation and Capture by Walls in a Particulate Aerosol Channel Flow*, Journal of Aerosol Science, 38:333-351, 2007.
4. Li, S.-Q. and J. S. Marshall, *Discrete Element Simulation of Micro-particle Deposition on a Cylindrical Fiber in an Array*, Journal of Aerosol Science, 38:1031-1046, 2007.
5. Zhao, Y. and J. S. Marshall, Spin *Coating of a Colloidal Suspension*, Physics of Fluids, 20:043302-1-15, 2008.
6. Wada, K., H. Tanaka, T. Suyama, H. Kimura, and T. Yamamoto, *Numerical Simulation of Dust Aggregation Collisions. I. Compression and Disruption of Two-dimensional Aggregates*, The Astrophysical Journal, 661:320-333, 2007.
7. Wada, K., H. Tanaka, T. Suyama, H. Kimura, and T. Yamamoto, *Numerical Simulation of Dust Aggregation Collisions. II. Compression and Disruption of Three-dimensional Aggregates in Head-on Collisions*, The Astrophysical Journal, 667:1296-1308, 2008.
8. Johnson, K. L., K. Kendall, and A. D. Roberts, *Surface Energy and the Contact of Elastic Solids*, Proceedings of the Royal Society of London A, 324:301-313, 1971.
9. Derjaguin, B. V., V. M. Muller, and YU. P. Toporov, *Effect of Contact Deformation and the Adhesion of Particles*, Journal of Colloid and Interface Science, 53:314-326.

10. Muller, V. M., V. S. Yushchenko, and B. V. Deraguin, *On the Influence of Molecular Forces on the Deformation of an Elastic Sphere and Its Sticking to a Rigid Plane*, Journal of Colloid and Interface Science, 77:91-101, 1980.
11. Muller, V. M., V. S. Yushchenko, and B. V. Deraguin, *General Theoretical Consideration of the Influence of Surface Forces on the Contact Deformations and the Reciprocal Adhesion of Elastic Spherical Particles*, Journal of Colloid and Interface Science, 92:92-101, 1983.
12. Tsai, C.-J., D. Y. H. Pui, and B. Y. H. Liu, *Elastic Flattening and Particle Adhesion*, Aerosol Science and Technology, 15:239-255, 1991.
13. Silbert, L., D. Ertaş, G. S. Grest, T. C. Halsey, D. Levine, and S. J. Plimpton, *Granular Flow Down an Inclined Plane: Bagnold Scaling and Rheology*, Physical Review E, 64:051302-1-14, 2001.
14. Brilliantov, N., F. Spahn, J.-M. Hertzsch, and T. Pöschel, *Model for Collisions in Granular Gases*, Physical Review E, 53:5382-5392, 1996.
15. Tsuji, Y., T. Tanaka, and T. Ishida, *Lagrangian Numerical Simulation of Plug Flow of Cohesionless Particles in a Horizontal Pipe*, Powder Technology, 71:239-250, 1992.
16. Meakin, P., *Fractal Aggregates in Geophysics*, Reviews of Geophysics, 29:317-354, 1991.
17. Witten, T. A. and M. E. Cates, *Tenuous Structures from Disorderly Growth Processes*, Science, 1607-1612, June 27, 1986.
18. Jullien, R., *Transparency Effects in Cluster-Cluster Aggregation with Liner Trajectories*, Journal of Physics A: Mathematical and General, 17:L771-L776, 1984.
19. Kempf, S., S. Pfalzner, and T. K. Henning, *N-particle-simulations of Dust Growth I. Growth Driven by Brownian Motion*, Icarus, 141:388-398, 1999.
20. Kempf, S. and S. Pfalzner, *An Effective Algorithm for Simulating Diffusion-driven Aggregation*. Computer Physics Communications, 137:225-235, 2001.

DISTRIBUTION

1	MS0736	Dana A. Powers	6770
1	MS0747	Veena Tikare	6774
1	MS1303	Gary S. Grest	1114
2	MS9018	Central Technical Files	8944
2	MS0899	Technical Library	9536

Sandia National Laboratories